Quantum superpositions of clockwise and counterclockwise supercurrent states in the dynamics of an rf-SQUID exposed to a quantized electromagnetic field

R. Migliore* and A. Messina

INFM and MIUR, Dipartimento di Scienze Fisiche ed Astronomiche dell'Università di Palermo, via Archirafi 36, 90123 Palermo, Italy

(Received 18 November 2002; revised manuscript received 3 February 2003; published 3 April 2003)

The dynamical behavior of a superconducting quantum interference device (an rf-SQUID) irradiated by a single-mode quantized electromagnetic field is theoretically investigated. Treating the SQUID as a flux qubit, we analyze the dynamics of the combined system within the low-lying energy Hilbert subspace both in the asymmetric and in the symmetric SQUID potential configurations. We show that the temporal evolution of the system is dominated by an oscillatory behavior characterized by more than one, generally speaking, incommensurable Rabi frequencies whose expressions are explicitly given. We find that the external parameters may be fixed in such a way to realize a control on the dynamical replay of the total system which, for instance, may be forced to exhibit a periodic evolution accompanied by the occurrence of an oscillatory disappearance of entanglement between the two subsystems. We demonstrate the possibility of generating quantum maximally entangled superpositions of the two macroscopically distinguishable states describing clockwise and counterclockwise supercurrents in the loop. The experimental feasibility of our proposal is briefly discussed.

DOI: 10.1103/PhysRevB.67.134505 PACS number(s): 85.25.Dq, 03.67.Lx

I. INTRODUCTION

It is of great interest to understand and study the physics of Josephson junction-based devices both for testing fundamental properties of quantum mechanics, such as the superposition principle or the occurrence of entangled states,[1] and for technological applications in context of quantum information theory and quantum computing.[2]

In the last decade, rapid developments in the realm of nanotechnologies have made it possible to perform a number of interesting and sophisticated experiments at low temperature,[3] bringing to light the existence in these *atomlike* circuits of many macroscopic quantum phenomena such as energy-level quantization,[4] macroscopic quantum tunneling, and quantum superposition of states.[5,6] More recently, the usefulness of investigating these solid-state devices in the context of quantum communication and information theory has been fully recognized.

Superconducting Josephson devices may, in fact, be thought of as two-state systems realizing the elementary unit of quantum information, known as quantum bit or qubit.[7] Moreover, Josephson devices can be scaled up to a large number of qubits and their dynamics may be controlled by externally applied voltages and magnetic fluxes. Superconducting devices such as Cooper pair boxes, Josephson junctions (JJ's), or super conducting quantum interference devices (SQUID's) have been thus proposed and used as basic elements for the practical realization of quantum gates and chips.[8] The relevant macroscopic degree of freedom, allowing to store and manipulate quantum information, may be the charge on the island of a Cooper pair box or the phase difference at the junction. In the first case, the charging energy E_C overcomes the Josephson energy E_J. Otherwise, in the opposite regime, the Josephson energy overcomes E_C.[9] It has been already experimentally demonstrated that Cooper pair boxes behave as two-level systems which can be coherently controlled[10–12] and now great efforts are devoted to prove that the same can be done with flux and phase qubits.[5,6,13] However, successful realization of quantum algorithms critically depends on the ability to entangle quantum states of qubits. The optimum would be the realization of a tunable coupling bus. Several coupling mechanisms are possible but the natural way of coupling two or more superconducting qubits is through an intermediate *resonant LC circuit*, playing the role of a data bus.[14,15] Such a resonant LC circuit, describable as a quantum harmonic oscillator, may be, in principle, replaced by the electromagnetic single-mode of a high-Q cavity or by a large-area current biased Josephson junction. In all these cases, the situation is similar to cavity QED (Ref. 16) (where cavity and atoms play the roles of the LC circuit and qubits, respectively) and to ion-trap proposals.[17]

It is then evidently of interest to study the interaction between a two-level solid-state system, such as an rf-SQUID, and an external quantum system–like another qubit, a tank circuit or a monochromatic radiation source.[15,18–24] The aim of such investigations is to bring to light the occurrence of entangled states and to construct coupling schemes by which the coherent dynamics of the system may be controlled and/or manipulated.[10,12–14,25–27]

In this paper, our main scope is to study the dynamics of a flux qubit (an rf-SQUID) coupled to a single-mode quantized electromagnetic field of a resonant cavity. Confining ourselves to the low-lying energy Hilbert space, we prove that the time evolution of the combined system is characterized by the occurrence of entanglement that may be controlled in terms of the strength of the coupling and the circuit parameters. In addition, we show that the dynamics is dominated by an oscillatory behavior traceable back to the existence of a finite set of characteristic Rabi frequencies whose expression may be explicitly given.

The importance of conceiving experimental schemes for realizing quantum superpositions of macroscopically distinguishable states has been quite recently emphasized.[28] The main result of this paper is that, appropriately acting upon some control parameters, it is possible to guide the rf-SQUID toward coherent maximally entangled combinations of two states describing clockwise and counterclockwise su-

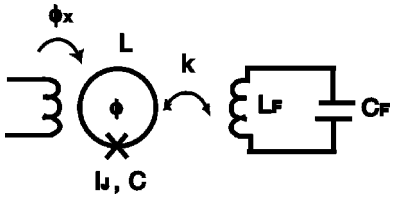

FIG. 1. Schematics of the superconducting circuits with a flux qubit inductively coupled to an *LC* resonator modeling a single-mode quantized electromagnetic field of a resonant high-*Q* cavity.

percurrents and then macroscopically distinguishable.

In Sec. II, we describe the physical system under study. Its dynamics in a reduced low-lying energy Hilbert space is studied in Sec. III where the main results of this paper are reported. In Sec. IV, we discuss our results and we conclude with some remarks about the feasibility of an experiment aimed at verifying our theory in the laboratory.

II. THE QUANTUM CIRCUIT

In this section, we describe in detail the physical system, namely, an rf-SQUID coupled to a monochromatic field of a high-*Q* resonant cavity and its Hamiltonian model. In Fig. 1 the electromagnetic single-mode cavity is represented as an LC resonator.

In Sec. II A, we describe the physical conditions that allow us to consider a SQUID as a two-level system, that is, as a flux qubit. Then we give the Hamiltonian model for the cavity field in terms of the combined system characteristics and finally, in Sec. II C, we consider the inductive coupling between these two subsystems.

A. The rf-SQUID as material two-level system

Let us begin by describing as usual[9] the rf-SQUID, a superconducting loop interrupted by a Josephson junction [Fig. 2(a)], as a fictitious particle of mass C and generalized coordinate ϕ (the magnetic flux in the loop) subjected to the washboard potential

$$U(\phi)=-E_J\cos\left(2\pi\frac{\phi}{\phi_0}\right)+\frac{(\phi-\phi_x)^2}{2L}, \tag{1}$$

where $C\sim10^{-15}$–10^{-13} F is the junction capacitance, $L\sim10$–100 pH the self-inductance of the loop, ϕ_x an externally applied dc flux, and $\phi_0=h/2e$ the flux quantum. The Josephson coupling energy E_J is related to the critical supercurrent I_C by $E_J=I_C\phi_0/2\pi$.

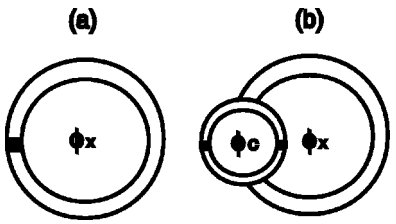

FIG. 2. (a) Schematics of an rf-SQUID and (b) of a double rf-SQUID obtained replacing the single Josephson junction with a dc-SQUID, namely, a superconducting loop interrupted by two Josephson junctions.

Taking into account both the kinetic and the potential energy, it is then immediate to write the Hamiltonian of the system as follows:

$$H=\frac{Q^2}{2C}-E_J\cos\left(2\pi\frac{\phi}{\phi_0}\right)+\frac{(\phi-\phi_x)^2}{2L}, \tag{2}$$

where the charge on the junction capacitance $Q=-i\hbar\partial/\partial\phi$ and the flux ϕ in the loop are canonically conjugate operators satisfying the commutation rule $[\phi,Q]=i\hbar$. Under the condition $\beta_L=2\pi LI_C/\phi_0>1$, the rf-SQUID is hysteretic and the potential $U(\phi)$ may have one or several relative minima. The height of barrier between minima and the number of minima depends on the parameter β_L. The form of the potential $U(\phi)$ instead can be tuned by changing the external dc magnetic flux ϕ_x applied to the loop to the case where the two lowest-energy wells are degenerate. This case occurs for $\phi_x=\phi_0/2$. These two degenerate minima correspond to the clockwise and counterclockwise sense of rotation of the supercurrent in the loop. The two relative ground states are localized flux states, hereafter denoted $|L\rangle$ and $|R\rangle$. For ϕ_x not exactly coincident with $\phi_0/2$, $U(\phi)$ defines an asymmetric double-well potential near $\phi=\phi_0/2$ with barrier V_b between these two lowest-energy minima. At sufficiently low temperatures, transitions between neighboring flux states are dominated by macroscopic quantum tunneling. However, for high barrier V_b, tunneling does not mix the two lowest-flux states with the excited states in the two wells. Thus, in the parameter regime $V_b\gg\hbar\omega_0\gg k_BT$ ($\hbar\omega_0$ being the separation of the first excited state from the ground state in both wells), the rf-SQUID effectively behaves as a two-state system[7] with reduced Hamiltonian expressible in terms of the Pauli matrices σ_x and σ_z as follows:

$$H_S=-\frac{\hbar}{2}\Delta\sigma_x+\frac{\hbar}{2}\epsilon\sigma_z=\frac{\hbar}{2}\begin{pmatrix}\epsilon & -\Delta\\ -\Delta & -\epsilon\end{pmatrix}, \tag{3}$$

where the basis coincides with the two localized flux states $|L\rangle$ and $|R\rangle$. Here $\hbar\epsilon(\phi_x)\equiv\hbar\epsilon=2I_C\sqrt{6(\beta_L-1)}(\phi_x-\phi_0/2)$ is the asymmetry of the double well and Δ is the tunneling frequency between the wells. This tunneling frequency can be tuned by changing the height V_b of the barrier that depends on the Josephson coupling energy E_J. Then if we replace the junction by a hysteretic dc-SQUID [Fig. 2(b)], behaving as a JJ with tunable critical current, E_J may be manipulated by a separate control dc flux ϕ_c. In other words, this modified device, known as the double rf-SQUID, behaves as a normal rf-SQUID whose Josephson energy E_J is related to the control flux ϕ_c by $E_J(\phi_c)=(\phi_0/\pi)I_{C0}\cos[\pi(\phi_c/\phi_0)]$, I_{C0} being the critical current of each of the two JJ's of the dc-SQUID.

Since in our scheme we need to control Δ, in what follows we will investigate a double rf-SQUID with two external control fluxes ϕ_x and ϕ_c when it is exposed to a monochromatic quantized electromagnetic field.

The Hamiltonian of the double rf-SQUID, given also in this case by Eq. (3), can be easily cast in diagonal form

$$H_S=\frac{\hbar}{2}\begin{pmatrix} -\sqrt{\epsilon^2+\Delta^2} & 0 \\ 0 & \sqrt{\epsilon^2+\Delta^2} \end{pmatrix} \tag{4}$$

in the basis formed by its eigenstates $|\sigma\rangle$ ($\sigma\equiv\mp$) given by

$$|-\rangle=C_-\left[|R\rangle+\frac{\epsilon+\sqrt{\epsilon^2+\Delta^2}}{\Delta}|L\rangle\right] \tag{5}$$

and

$$|+\rangle=C_+\left[|R\rangle+\frac{\epsilon-\sqrt{\epsilon^2+\Delta^2}}{\Delta}|L\rangle\right]. \tag{6}$$

Here $C_\mp=(1+[(\epsilon\pm\sqrt{\epsilon^2+\Delta^2})/\Delta]^2)^{-1/2}$ are the normalizing factors of $|-\rangle$ and $|+\rangle$, respectively, and $\hbar\sqrt{\epsilon^2+\Delta^2}$ is the energy difference between their corresponding eigenvalues $E_-=-(\hbar/2)\sqrt{\epsilon^2+\Delta^2}$ and $E_+=(\hbar/2)\sqrt{\epsilon^2+\Delta^2}$.

B. The quantized electromagnetic field

In this section, we model the electromagnetic field of the resonant cavity as an LC resonator. In this way our treatment and our results may be easily extended to the case of the coupling between the flux qubit and a real LC resonator[21] or a large-area current-biased Josephson junction.[13,15] This fact is important because, in order to verify experimentally our theoretical predictions, it is more practical to couple the qubit with one of these two systems rather than with the single mode of a resonant cavity. We therefore start by considering the Hamiltonian of an L_FC_F resonator with infinite parallel resistance on resonance and frequency $\omega_F=1/\sqrt{L_FC_F}$

$$H_F=\frac{Q_F^2}{2C_F}+\frac{\phi_F^2}{2L_F}, \tag{7}$$

where ϕ_F and Q_F play the roles of the magnetic flux and charge operators arising from the quantized electromagnetic field and satisfying the commutation rule $[\phi_F,Q_F]=i\hbar$.

As in Refs. 18 and 20, it is possible to relate the resonator operators ϕ_F and Q_F to bosonic annihilation and creation operators a and $a^\dagger$. Defining the flux ϕ_F and the conjugate operator Q_F as

$$\phi_F=\sqrt{\frac{\hbar}{2\omega_FC_F}}(a+a^\dagger) \tag{8}$$

and

$$Q_F=-i\sqrt{\frac{\hbar\omega_FC_F}{2}}(a-a^\dagger) \tag{9}$$

and substituting these analytical expressions in Eq. (7), it is immediate to cast the Hamiltonian of the resonator in the form of a standard harmonic-oscillator free Hamiltonian

$$H_F=\hbar\omega_F\left(a^\dagger a+\frac{1}{2}\right). \tag{10}$$

Here, the frequency ω_F, choosing $C_F\sim10^{-12}$ F and $L_F\sim0.1$ nH, belongs in the range of microwaves ($\omega_F\approx10^{11}$ rad s^{-1}). The eigenfunctions of Hamiltonian (10) are, of course, harmonic-oscillator eigenstates $|n\rangle$ (defined by $a^\dagger a|n\rangle=n|n\rangle$) with eigenvalues $E_n=\hbar\omega_F(n+\frac{1}{2})$.

If the rf-SQUID is effectively coupled with the quantized mode of an electromagnetic high-Q cavity, we may start again from Hamiltonian (7). In order to understand the meaning of C_F in this case, we assume that the rf-SQUID is located perpendicularly to the magnetic field and within a distance small as compared to the radiation wavelength. In such conditions, the vector potential $\mathbf{A}(\mathbf{x})$ arising from the electromagnetic field of the cavity mode is approximately uniform throughout the region of the device and in international units and in the Coulomb gauge ($\nabla\cdot\mathbf{A}=0$), it assumes the form

$$\mathbf{A}=\left(\frac{\hbar}{2\epsilon_0\omega_FV}\right)^{1/2}(a-a^\dagger)\,\mathbf{u}, \tag{11}$$

$\mathbf{u}$ being the unit polarization vector, ϵ_0 the vacuum dielectric constant, and V the quantization volume of the field mode. Thus, the expression for the operator ϕ_F to be inserted in Eq. (7) may be written down as

$$\phi_F=\oint_\gamma\mathbf{A}\cdot d\mathbf{l}=\sqrt{\frac{\hbar}{2\omega_FC_F}}\,(a+a^\dagger), \tag{12}$$

where the capacitive parameter C_F given by the following expression:

$$C_F=\epsilon_0V\left(\oint_\gamma\mathbf{u}\cdot d\mathbf{l}\right)^{-2} \tag{13}$$

depends on the field frequency, via the quantization volume V, and on the SQUID geometry, via the line integral which is taken across a closed circuit γ inside the SQUID loop. Then, also in this case, exploiting Eq. (12) and the properties of conjugation between ϕ_F and Q_F, it is easy to cast Hamiltonian (7) in the form of a standard harmonic-oscillator free Hamiltonian (10).

C. The coupled system

In view of the assumptions made in the preceding section, the flux qubit and the LC-resonator modeling the monochromatic field can be thought of as coupled together inductively (see Fig. 1) with a contribution to the total Hamiltonian given by

$$H_I=\frac{2k}{L}\phi\phi_F=B(a+a^\dagger)[-\epsilon\sigma_z+\Delta\sigma_x]=H_{RWA}+H_{res} \tag{14}$$

with

$$H_{RWA}=B\Delta(a\sigma_++a^\dagger\sigma_-), \tag{15}$$

$$H_{res}=B\Delta(a^\dagger\sigma_++a\sigma_-)-B(a+a^\dagger)\epsilon\sigma_z, \tag{16}$$

and where the constant

$$B=\frac{k}{L}\sqrt{\frac{\hbar}{2\omega_F C_F}}\frac{\phi_0}{\sqrt{\epsilon^2+\Delta^2}} \tag{17}$$

has the same dimension of $\hbar$ and depends on the coupling strength and the system characteristics. Here, the flux linkage factor k is assumed of the order of 0.01 in accordance with the current experimental values.[29] Thus, the Hamiltonian describing our weakly interacting rf-SQUID-field system can be written down as

$$H=H_S+H_F+H_I, \tag{18}$$

where H_S and H_F, given by Eqs. (4) and (10), are the Hamiltonians describing the two free subsystems.

III. THE SYSTEM DYNAMICS IN A REDUCED LOW-LYING ENERGY FOUR-DIMENSIONAL (4D) HILBERT SUBSPACE

In view of Eqs. (4), (10), and (14), the Hamiltonian H may be formally interpreted as that of a two-level ''atom'' quantum mechanically interacting with a monochromatic quantized electromagnetic field. We wish to focus our attention on a physical situation wherein the operating temperature is $T\approx 10$ mK and the field is in resonance with the transition between the lowest and the first excited state of the rf-SQUID, that is, $\hbar\omega_F=\hbar\sqrt{\epsilon^2+\Delta^2}$. It is well known that in such conditions, the dynamical contribution of the rotating terms of Hamiltonian (18) is preponderant in comparison to that from H_{res}. To carry forward our dynamical analysis we could at this point ignore H_{res} in H_I confining ourselves into a Jaynes-Cummings (JC) like model as other authors do.[14] Instead, we wish to investigate the effects stemming from H_{res}. As a consequence, we have to circumvent the very difficult problem of diagonalizing H in its infinite-dimensional Hilbert space. To this end we focus our attention on the time evolution of the combined system when it starts from the condition $|n\sigma\rangle\equiv|n\rangle|\sigma\rangle$ such that no more than one matter-radiation excitation $[n+(\sigma+1/2)$ with $\sigma\equiv\pm 1]$ is present. Under this initial condition and considering the predominance of H_{RWA} on H_{res}, one may guess that most of the evolution occurs within the low-lying energy subspace of the free Hamiltonian $H_0=H_S+H_F$ spanned by the four states $|n\sigma\rangle$, with $n\equiv 0,1$ and $\sigma\equiv -,+$. This physical expectation is confirmed by numerical simulations we have performed on a bigger Hilbert space generated by the 12 states $|n\sigma\rangle$, with $n\equiv 0,1,\ldots,5$ and $\sigma\equiv -,+$.

Putting together all these considerations, in what follows we will study the dynamics of the coupled matter-radiation system, both in the asymmetric ($\epsilon\neq 0$) and symmetric ($\epsilon=0$) case, using as starting point the reduced Hamiltonian

$$H_R=\begin{pmatrix} 0 & -B\epsilon & 0 & B\Delta \\ -B\epsilon & \hbar\omega_F & B\Delta & 0 \\ 0 & B\Delta & \hbar\omega_F & B\epsilon \\ B\Delta & 0 & B\epsilon & 2\hbar\omega_F \end{pmatrix} \tag{19}$$

from initial conditions having at most one matter-radiation excitation.

A. The dynamics of the system in the asymmetric case

Let us consider the time evolution of the combined rf-SQUID-radiation system initially prepared in the state $|0+\rangle$, that is, the field in its vacuum state $|0\rangle$ and the SQUID in the first excited state $|+\rangle=C_+[|R\rangle+(\epsilon-\sqrt{\epsilon^2+\Delta^2}/\Delta)|L\rangle]$, which is a superposition of the localized flux states $|L\rangle$ and $|R\rangle$.

It is worth noting that the manipulation of the shape of the potential and the height of the barrier between the two lowest-energy wells via the control fluxes ϕ_x and ϕ_c allows to prepare the SQUID in a prefixed initial condition.[8,29] At the same time, exploiting the currently available experimental techniques in CQED, it is possible to prepare the field mode in a Fock state with 0 or 1 photon.[16] Eigenvalues $|u_i\rangle$ $(i\equiv 1,2,3,4)$ and eigenvectors λ_i of H_R in the asymmetric case may be exactly evaluated and they are explicitly given in Appendix A.

The expansion of $|0+\rangle_t=\exp[-i(H_R t/\hbar)]|0+\rangle$ in terms of $|u_1\rangle$, $|u_2\rangle$, $|u_3\rangle$, and $|u_4\rangle$ may be cast in the following form:

$$\begin{aligned}|0+\rangle=\frac{B\epsilon}{(P_1-P_2)Q_1Q_2}[&\sqrt{n_1}(P_2-Q_1)Q_2|u_1\rangle\exp(-i\lambda_1 t)\\&-\sqrt{n_2}(P_2+Q_1)Q_2|u_2\rangle\exp(-i\lambda_2 t)\\&-\sqrt{n_3}(P_1-Q_2)Q_1|u_3\rangle\exp(-i\lambda_3 t)\\&+\sqrt{n_4}(P_1+Q_2)Q_1|u_4\rangle\exp(-i\lambda_4 t)].\end{aligned} \tag{20}$$

Thus, $|0+\rangle$ is as in linear superposition, with different weights, of the eigenstates $|u_i\rangle$ of Hamiltonian (19).

We are interested in exploring the ability of the system to periodically come back to the initial state $|0+\rangle$ as well as to pass through the other states $|1-\rangle$, $|0-\rangle$, and $|1+\rangle$. The structure of the previous equation and those of Eqs. (A10)–(A13) make clear that the time evolution of the system from $|0+\rangle$ involves all the four states $|0-\rangle$, $|1-\rangle$, $|0+\rangle$, and $|1+\rangle$. However, since the states $|0+\rangle$ and $|1-\rangle$ are almost degenerate in energy, in our physical situation transitions between them are more probable than transitions between the initial state $|0+\rangle$ and the states $|0-\rangle$ and $|1+\rangle$. This fact may be clearly appreciated by evaluating the time evolution of the survival probability $P_1(t)$ of the state $|0+\rangle$, that is,

$$\begin{aligned}P_1(t)=|\langle 0+|0+\rangle_t|^2=S^2\Bigg\{&\sum_{j=1}^{4}S_j^2+2S_1S_2\cos\frac{Q_1}{\hbar}t\\&+2S_3S_4\cos\frac{Q_2}{\hbar}t+2[S_1S_3+S_2S_4]\cos\frac{(Q_1-Q_2)}{2\hbar}t\\&+2[S_2S_3+S_1S_4]\cos\frac{(Q_1+Q_2)}{2\hbar}t\Bigg\},\end{aligned} \tag{21}$$

where

$$S=\frac{B\epsilon}{(P_1-P_2)Q_1Q_2}, \tag{22}$$

$$S_1=\frac{P_1Q_2}{2B\epsilon}(Q_1-P_2), \tag{23}$$

$$S_2=\frac{P_1Q_2}{2B\epsilon}(Q_1+P_2), \tag{24}$$

$$S_3=-\frac{P_2Q_1}{2B\epsilon}(Q_2-P_1), \tag{25}$$

and

$$S_4=-\frac{P_2Q_1}{2B\epsilon}(Q_2+P_1). \tag{26}$$

It is immediate to construct explicit expressions also for the transition probabilities $P_2(t)=|\langle 1-|0+\rangle_t|^2$, $P_3(t)=|\langle 0-|0+\rangle_t|^2$, and $P_4(t)=|\langle 1+|0+\rangle_t|^2$ to the states $|1-\rangle$, $|0-\rangle$, and $|1+\rangle$, respectively. Their explicit analytical expressions are given in Appendix B. Here we wish to underline that these transition probabilities have the same mathematical structure of Eq. (21). This means that P_2, P_3, and P_4 like P_1 are given by the sum of a constant and four trigonometric time-dependent terms with different weights and frequencies. Since these four frequencies $\omega_1\equiv Q_1/\hbar$, $\omega_2\equiv Q_2/\hbar$, $\omega_3\equiv(Q_1-Q_2)/2\hbar$ and $\omega_4\equiv(Q_1+Q_2)/2\hbar$ appearing in the expressions of $P_1(t)$, $P_2(t)$, $P_3(t)$, and $P_4(t)$ are in general incommensurable, we find a quasiperiodic behavior wherein a complete exact inversion of the populations between the degenerate states $|0+\rangle$ and $|1-\rangle$ never occurs. The time evolutions of P_1, P_2, P_3, and P_4 are plotted in Fig. 3.

A similar quasiperiodic behavior characterizes the time evolution of the system initially prepared in the state $|0R\rangle=|0\rangle\otimes|R\rangle$, that is, the field in the vacuum state $|0\rangle$ and the rf-SQUID in the localized flux state $|R\rangle$ characterized by a well-defined sense of circulation of the supercurrent in the loop. In view of the definitions of $|-\rangle$ and $|+\rangle$ as well as of Eqs. (A14) and (A16), the survival probability of the state $|0R\rangle$ can be cast in the following form:

$$\begin{aligned}P_{0R}(t)&=|\langle 0R|0R\rangle_t|^2\\&=W^2\Bigg\{\sum_{j=1}^{4}W_j^2+2W_1W_2\cos\frac{Q_1}{\hbar}t+2W_3W_4\cos\frac{Q_2}{\hbar}t\\&\quad+2[W_1W_3+W_2W_4]\cos\frac{(Q_1-Q_2)}{2\hbar}t\\&\quad+2[W_2W_3+W_1W_4]\cos\frac{(Q_1+Q_2)}{2\hbar}t\Bigg\},\end{aligned} \tag{27}$$

where now

$$W=\frac{B}{(P_1-P_2)Q_1Q_2}, \tag{28}$$

$$W_1=Q_2[\epsilon\delta_+(P_2-Q_1)+P_2\Delta\delta_-]\times\left(-\frac{P_2+Q_1}{2B\Delta}\delta_--\frac{P_1}{2B\epsilon}\delta_+\right), \tag{29}$$

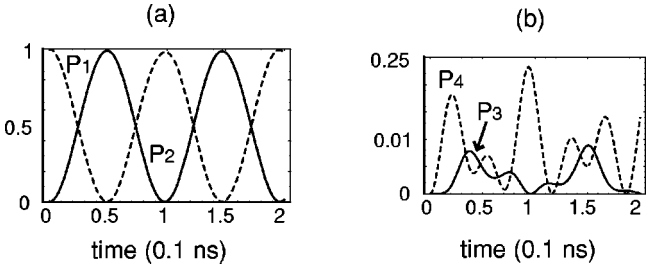

FIG. 3. (a) Survival probability P_1 of the state $|0+\rangle$ (dashed line) and transition probabilities P_2, (b) P_3 and P_4 (dashed line) to the states $|1-\rangle$, $|0-\rangle$, and $|1+\rangle$, respectively, for a system with $\epsilon\approx 3\times 10^{10}$ rad s^{-1}, $B\approx 2{,}7\times 10^{-35}$ J s and $\omega_F\approx 10^{11}$ rad s^{-1}.

$$W_2=-Q_2[\epsilon\delta_+(P_2+Q_1)+P_2\Delta\delta_-]\times\left(\frac{-P_2+Q_1}{2B\Delta}\delta_--\frac{P_1}{2B\epsilon}\delta_+\right), \tag{30}$$

$$W_3=Q_1[\epsilon\delta_+(-P_1+Q_2)-P_1\Delta\delta_-]\times\left(-\frac{P_1+Q_2}{2B\Delta}\delta_--\frac{P_2}{2B\epsilon}\delta_+\right), \tag{31}$$

$$W_4=Q_1[\epsilon\delta_+(P_1+Q_2)+P_1\Delta\delta_-]\times\left(-\frac{P_1-Q_2}{2B\Delta}\delta_--\frac{P_2}{2B\epsilon}\delta_+\right), \tag{32}$$

and $\delta_\pm=(\sqrt{\epsilon^2+\Delta^2}\pm\epsilon)/2C_\pm\sqrt{\epsilon^2+\Delta^2}$. Figure 4 displays this survival probability as well as the transition probabilities $P_{0L}(t)=|\langle 0L|0R\rangle_t|^2$ [dashed line in Fig. 4(a)], $P_{1R}(t)=|\langle 1R|0R\rangle_t|^2$, and $P_{1L}(t)=|\langle 1L|0R\rangle_t|^2$ [dashed line in Fig. 4(b)] to the states $|0L\rangle$, $|1R\rangle$, and $|1L\rangle$, respectively. Also in this case we underline that the time evolution of all these transition probabilities is governed by the four characteristic frequencies ω_1, ω_2, ω_3, and ω_4 previously defined.

This leads to a very rich dynamics of the system, characterized by the occurrence of entangled states of the total coupled system obtained by the superposition of states with opposite sense of circulation of the supercurrent in the loop and a different number of photons in the field (0 or 1). However, due to the fact that these characteristic frequencies are not rationally related to each other, it is impossible to restore exactly the initial condition of the system. As we will

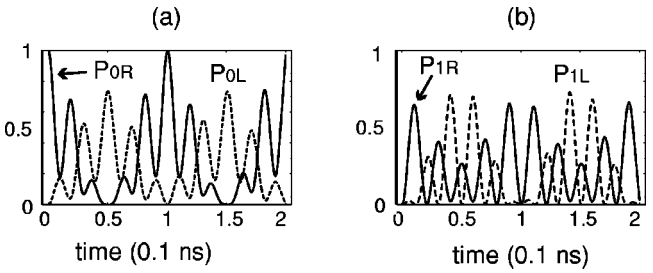

FIG. 4. (a) Survival probability P_{0R} of the state $|0R\rangle$ and transition probabilities P_{0L} (dashed line), (b) P_{1R} and P_{1L} (dashed line) to the states $|0L\rangle$, $|1R\rangle$, and $|1L\rangle$, respectively, for a system with $\epsilon\approx 3\times 10^{10}$ rad s^{-1}, $B\approx 10^{-34}$ J s, and $\omega_F\approx 10^{11}$ rad s^{-1}.

show in the following section, it is possible to find an exact correspondence between these frequencies and then a more regular behavior for the total system, in the symmetric case and choosing properly the values of the coupling strength k and of the system parameters.

B. The dynamics of the system in the symmetric case: Existence of quantum superpositions of clockwise and counterclockwise supercurrent states

In the previous case, the asymmetric SQUID potential configuration results from the application of a dc control flux ϕ_x not exactly equal to $\phi_0/2$. In this section, we will study the system when $\phi_x=\phi_0/2$. This means that the two SQUID potential wells have the same height so that $\epsilon=0$. In such symmetric conditions, Hamiltonian (19) reduces to the relatively simpler form

$$H_R=\begin{pmatrix} 0 & 0 & 0 & B\Delta \\ 0 & \hbar\omega_F & B\Delta & 0 \\ 0 & B\Delta & \hbar\omega_F & 0 \\ B\Delta & 0 & 0 & 2\hbar\omega_F \end{pmatrix}, \tag{33}$$

where B must be calculated putting $\epsilon=0$ in Eq. (17).

Analyzing the structure of matrix (33), it is not difficult to convince oneself that there exist two dynamically separated subspaces, characterized by the frequencies $\Omega_1=(B/\hbar)\omega_F$ and $\Omega_2=\sqrt{\hbar^2+B^2}/\hbar\omega_F$, respectively. The first subspace is generated by $|0+\rangle$ and $|1-\rangle$ and the representation of H_R on it is given by the central 2×2 matrix block. Such a structure is responsible of the appearance of entanglement in the time evolution of the combined rf-SQUID-field system. The matrix elements of H connecting the states $|0-\rangle$ and $|1+\rangle$ generating the second subspace reflect the contribution of counterrotating terms in the truncated version of H.[24]

The eigenstates of matrix (33) assume the simple form

$$|u_{1s}\rangle=\frac{1}{\sqrt{2}}[-|1-\rangle+|0+\rangle], \tag{34}$$

$$|u_{2s}\rangle=\frac{1}{\sqrt{2}}[|1-\rangle+|0+\rangle], \tag{35}$$

$$|u_{3s}\rangle=\frac{1}{\sqrt{n_{3s}}}\left[-\frac{(\hbar+\sqrt{B^2+\hbar^2})}{B}|0-\rangle+|1+\rangle\right], \tag{36}$$

$$|u_{4s}\rangle=\frac{1}{\sqrt{n_{4s}}}\left[-\frac{(\hbar-\sqrt{B^2+\hbar^2})}{B}|0-\rangle+|1+\rangle\right], \tag{37}$$

with eigenvalues given by

$$\lambda_{1s}=(\hbar-B)\ \ \omega_F, \tag{38}$$

$$\lambda_{2s}=(\hbar+B)\ \ \omega_F, \tag{39}$$

$$\lambda_{3s}=(\hbar-\sqrt{B^2+\hbar^2})\ \ \omega_F, \tag{40}$$

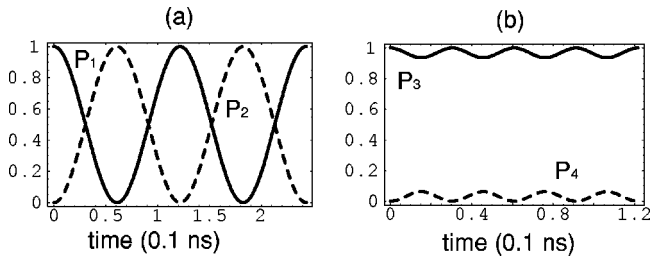

FIG. 5. (a) Survival probability P_1 and transition probability P_2 (dashed line) at the state $|1-\rangle$ for a system initially prepared in the state $|0+\rangle$. (b) Survival probability P_3 and transition probability P_4 (dashed line) at the state $|1+\rangle$ for a system initially prepared in the state $|0-\rangle$. In both cases, we set $\epsilon=0$, $B\approx2{,}7\times10^{-35}$ J s and $\omega_F\approx10^{11}$ rad s^{-1}.

$$\lambda_{4s}=(\hbar+\sqrt{B^2+\hbar^2})\ \ \omega_F. \tag{41}$$

Expressions (34)–(37) and (38)–(41) may be immediately derived from those relative to the asymmetric case given in Appendix A in the limit for $\epsilon=0$. The two eigenstates $|u_{1s}\rangle$ and $|u_{2s}\rangle$ describe a maximum entangled condition of the rf-SQUID and the monochromatic field states, induced by the inductive coupling between them. Rabi oscillations between the degenerate states $|0+\rangle$ and $|1-\rangle$ dominate the dynamical behavior of the system whose time evolution may be written down as

$$|0+\rangle_t=\frac{1}{\sqrt{2}}[|u_{1s}\rangle\exp(-i\lambda_{1s}t/\hbar)+|u_{2s}\rangle\exp(-i\lambda_{2s}t/\hbar)] \tag{42}$$

if the initial condition $|0+\rangle$ is assumed. Also in this case we are interested in exploring the ability of the system to periodically come back to the initial state $|0+\rangle$ as well as to pass through the state $|1-\rangle$. To this end we plot both the survival probability $P_1(t)=|\langle0+|0+\rangle_t|^2=\frac{1}{2}(1+\cos2\Omega_1t)$ of the initial state [solid line in Fig. 5(a)] and the probability $P_2(t)=|\langle1-|0+\rangle_t|^2=\sin^2\Omega_1t$ to find the system in the state $|1-\rangle$ after a time t [dashed line in Fig. 5(a)]. Equation (42) together with Fig. 5(a) provides a clear evidence of the existence of coherent Rabi oscillations with frequency Ω_1 between the states $|0+\rangle$ and $|1-\rangle$ corresponding to the emission and absorption of a quantum of energy $\hbar\omega_F$ by the rf-SQUID.

Now let us consider the two-dimensional subspace in which the dynamics of the system, with respect to the truncated Hamiltonian (33), is governed only by the counterrotating terms with characteristic frequency Ω_2. Preparing the system in the state $|0-\rangle$ and considering its time evolution, we easily get

$$|0-\rangle_t=-\frac{B^2}{4(\hbar^2+B^2)}\left[\frac{1}{\sqrt{n_{4s}}}|u_{3s}\rangle\exp(-i\lambda_{3s}t/\hbar)-\frac{1}{\sqrt{n_{3s}}}|u_{4s}\rangle\exp(-i\lambda_{4s}t/\hbar)\right]. \tag{43}$$

Once more we calculate the survival probability $P_3(t) = |\langle 0-|0-\rangle_t|^2$ of the ground state $|0-\rangle$,

$$P_3(t) = \frac{B^2}{4(B^2+\hbar^2)}\left[\frac{4\hbar^2}{B^2} + 2(1-\cos 2\Omega_2 t)\right], \quad (44)$$

and the transition probability $P_4(t) = |\langle 1+|0-\rangle_t|^2$ to the state $|1+\rangle$,

$$P_4(t) = \frac{B^2}{2(B^2+\hbar^2)}[1-\cos 2\Omega_2 t]. \quad (45)$$

Analyzing the structure of these two expressions, we deduce that the entanglement between the two interacting subsystems leads to an oscillatory behavior as before, but now, as shown also in Fig. 5(b), we cannot get a complete population inversion between the ground state $|0-\rangle$ and the higher-energy excited state $|1+\rangle$. This is due to the fact that, in this reduced Hilbert space, processes involving the exchange of two quanta of energy between the two subsystems are unlikely.

Until now we have considered the system initially prepared in a state belonging to one of the two dynamically independent two-dimensional subspaces. In the following, we wish to consider richer physical situations involving both the two subspaces at the same time.

Considering, in fact, as initial condition the state $|0R\rangle = |0\rangle\otimes|R\rangle$, namely, the field in its vacuum state $|0\rangle$ and the SQUID with a right-hand current in the loop, the system evolves in accordance with the following expression:

$$|0R\rangle_t = \alpha(t)|0R\rangle + \beta(t)|0L\rangle + \gamma(t)|1R\rangle + \delta(t)|1L\rangle. \quad (46)$$

The time-dependent parameters appearing in Eq. (46) are linear combinations of trigonometric functions characterized by the incommensurable frequencies Ω_1 and Ω_2. In this case the time evolution of the system is rather similar to that obtained in the asymmetric case. Generally speaking, this fact makes it impossible for the system to exactly restore its initial condition. Since the ratio Ω_2/Ω_1 may be controlled by acting upon the parameter B and then, at least, on one of the physical parameters appearing in its expression given by Eq. (17), we may wonder on what the dynamical properties of the system become in correspondence to special values of B. It is indeed immediate to see that for

$$B = \hbar/\sqrt{n^2-1}, \quad (47)$$

we get $\Omega_2 = n\ \Omega_1$, where $n>1$ is an arbitrary integer. Under such a controllable condition, the dynamics of the system is dominated by the occurrence of many interesting features. The four time-dependent parameters appearing in Eq. (46) assume the form

$$\alpha(\tau) = \frac{\exp(-i\tau\sqrt{n^2-1})}{2}\left(\cos\tau + \cos n\tau + i\frac{\sqrt{n^2-1}}{n}\sin n\tau\right), \quad (48)$$

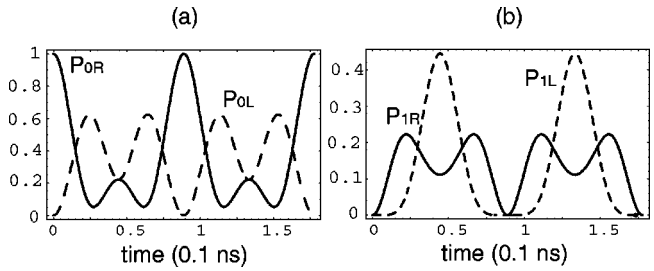

FIG. 6. (a) Survival probability of the state $|0R\rangle$ and transition probabilities to the states $|0L\rangle$ (dashed line), (b) $|1R\rangle$, and $|1L\rangle$ (dashed line) for a system initially prepared in the state $|0R\rangle$. Here, $n=3$, $\epsilon=0$, $B=\hbar/\sqrt{8}$, and $\omega_F \approx 10^{11}$ rad s^{-1}.

$$\beta(\tau) = \frac{\exp(-i\tau\sqrt{n^2-1})}{2} \times\left(-\cos\tau + \cos n\tau + i\frac{\sqrt{n^2-1}}{n}\sin n\tau\right), \quad (49)$$

$$\gamma(\tau) = -i\frac{\exp(-i\tau\sqrt{n^2-1})}{2}\left(\sin\tau + \frac{1}{n}\sin n\tau\right), \quad (50)$$

and

$$\delta(\tau) = -i\frac{\exp(-i\tau\sqrt{n^2-1})}{2}\left(\sin\tau - \frac{1}{n}\sin n\tau\right), \quad (51)$$

where $\tau = \Omega_1 t$. Analyzing the time evolution of these four time-dependent probability amplitudes, it is not difficult to convince oneself that *the system comes right back to the initial state* $|0R\rangle$ after a time $t_1 \equiv (2\pi/\Omega_1) = (2\pi\sqrt{n^2-1})/\omega_F$ if n is even and after a time $t_1/2$ if n is odd. For this reason, Eq. (47) expresses the condition for the occurrence of periodic behavior in the dynamics of the combined system.

Other interesting manifestations in the dynamics of the system occur depending on the parity of the ratio between Ω_2 and Ω_1 determined by the fixed value of B in accordance to Eq. (47).

We find indeed that, if n is even and always starting from the state $|0R\rangle$, at time $t_1/2$ the combined system reaches the factorized state wherein the field is still in its vacuum state $|0\rangle$ and the current in the loop reverses its sense of circulation, meaning that the state of the rf-SQUID becomes $|L\rangle$. If n is odd, on the contrary, the probability $P_{0L}(t)$ of finding the system in the state $|0L\rangle$ is always less than 1 [see, for example, for $n=3$ the dashed line in Fig. 6(a)].

Moreover, for n even, at times $t_1/4$ and $3t_1/4$, the system is once more describable in terms of factorized states. For example, for $n=4$ these factorized states may be expressed as

$$|\psi_0(t_1/4)\rangle = \frac{\exp(-i\pi\sqrt{15}/2)}{\sqrt{2}}[|0\rangle - i|1\rangle]\otimes|-\rangle, \quad (52a)$$

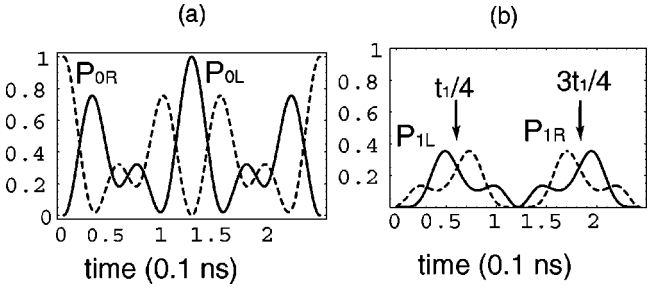

FIG. 7. (a) Survival probability of the state $|0R\rangle$ (dashed line) and transition probabilities to the states $|0L\rangle$, (b) $|1R\rangle$ (dashed line), and $|1L\rangle$ for a system initially prepared in the state $|0R\rangle$. Here, $n=4$, $\epsilon=0$, $B=\hbar/\sqrt{15}$, and $\omega_F \approx 10^{11}$ rad s^{-1}.

$$|\psi_0(3t_1/4)\rangle = \frac{\exp(-i3\pi\sqrt{15}/2)}{\sqrt{2}}[|0\rangle + i|1\rangle] \otimes |-\rangle, \tag{52b}$$

$|-\rangle$ being the ground state of the rf-SQUID. This coherent evolution is represented in Fig. 7 where we plot, for $n=4$, the survival probability $P_{0R}(t)$ of $|0R\rangle$ and the transition probabilities $P_{0L}(t)$, $P_{1R}(t)$, and $P_{1L}(t)$ to the states $|0L\rangle$, $|1R\rangle$, and $|1L\rangle$, respectively.

It has to be stressed that, on the contrary, when n is odd the previously described oscillations between factorized states and entangled states of the total matter-radiation system do not occur. This fact may be fully recognized looking at Fig. 6, where we plot $P_{0R}(t)$ $P_{0L}(t)$, $P_{1R}(t)$, and $P_{1L}(t)$ assuming $n=3$ and $P_{0R}(0)=1$. We note that a time instant in correspondence of which these four probabilities are all equal does not exist.

Remembering that $|-\rangle = 1/\sqrt{2}[|R\rangle + |L\rangle]$ and that the states $|R\rangle$ and $|L\rangle$ may be legitimately considered as macroscopically distinguishable states of the rf-SQUID, Eq. (52) predicts the generation of a maximally entangled Schrödinger catlike state in the dynamics of an rf-SQUID exposed to a single-mode quantized electromagnetic field when the combined system is prepared in the state $|0R\rangle$.

The fact of being able to build quantum superpositions of two states describing clockwise and counterclockwise supercurrents in the loop confirms the role of such nanodevices as simple physical systems due to which it is possible to conceive experiments on fundamental aspects of the quantum theory.

IV. DISCUSSION AND CONCLUSIVE REMARKS

In this paper we have investigated the coupled dynamics of an rf-SQUID and a single-mode quantized electromagnetic field in the reduced 4D Hilbert space spanned by the low-lying energy states of the uncoupled system. The correspondent Hamiltonian model includes contributions from both the rotating and counterrotating terms and this fact turns out to be at the origin of a rich dynamical behavior dominated by Rabi oscillations associated to more than one frequency. By construction, our theory is based on a Hamiltonian model containing some external parameters. Since they may be easily varied, we have addressed the interesting question of the extent at which this circumstance provides an effective tool to get a reasonable control of some aspects of the system dynamics. The analysis reported in the paper considers, fixing appropriate resonance conditions, two different cases, the asymmetric and the symmetric ones. In both cases, the dynamical problem is exactly solved in the truncated Hilbert space finding quasiperiodic behaviors of the initial state survival probability as well as of some physically meaningful transition probabilities of experimental interest. Such quasiperiodic temporal evolution reflects the existence of quantum coherent oscillations occurring at incommensurable Rabi frequencies. An important difference between the two physical situations under discussion is that in the symmetric case H_R exhibits two invariant 2D subspaces, whereas in the asymmetric case the time evolution of any initial condition of the total system explores the entire 4D Hilbert space. This different dynamical behavior has direct remarkable consequences. When indeed the external parameter ϵ measuring the height difference between the two minima of $U(\phi)$ does not vanish, the system evolves intrinsically preventing the occurrence of disentangling in correspondence to any possible choice of values for the external parameters. Our theory predicts completely different and rich results in the symmetric case stemming from the reducibility into 2×2 blocks of H_R in the truncated Hilbert space. We have, in fact, proved that the external parameters may be fixed in such a way to realize a control on the dynamical replay of the total system which, for instance, may be forced to exhibit a periodic evolution accompanied by the occurrence of an oscillatory disappearance of entanglement between the two subsystems. A relevant result of this paper is the generation of quantum superpositions of the two macroscopic distinguishable states $|L\rangle$ and $|R\rangle$ of the rf-SQUID when $\Omega_2 = n\ \Omega_1$, with n even.

It is worth noting that the sensitivity of these results to the parity of the ratio n between the characteristic frequency Ω_2 and Ω_1 is an effect of the counterrotating terms of Hamiltonian (19). The JC model, in fact, leads to the factorized states described by Eqs. (52). However, since in this case the dynamics of the system is driven only by the Rabi frequency $\Omega_1 = (B/\hbar)\omega_F$, we may obtain the factorized states (52) for any value of B.

These results are different and their value may be further appreciated considering that the realization of our theoretical scheme is in the grasp of experimentalists. The several types of SQUID necessary for the observability of our predictions are easily fabricated exploiting the well-defined trilayer $Nb/AlO_x/Nb$ technology. Moreover, it is possible to prepare and control the state of the rf-SQUID via flux pulses and rf pulses. Finally, we may readout the macroscopic flux state of the qubit using a suitable magnetometer (essentially an hysteretic dc-SQUID detector) whose experimentally measured detection efficiency is of the order of 98%.[30]

One of the most crucial problem related to this kind of device is the unavoidable presence of decoherence. The quality of coherence for a two-level system can be qualitatively described in terms of the coherence time T_φ of a superposition of its states. It is generally accepted that for an active decoherence compensation mechanism, T_φ must be larger

than $10^4 t_{op}$, t_{op} being the duration of an elementary operation of the qubit.[31] In our case the Rabi oscillation frequencies Ω_1 and Ω_2 correspond to characteristic times $t_1 \approx 2.4 \times 10^{-10}$ sec and $t_2 \approx 6 \times 10^{-11}$ sec (for $n=4$). Moreover, as demonstrated by Cosmelli and co-workers, for a system cooled at 5 mK and effective resistance $R \approx 4$–5 MΩ, the decoherence time is approximately of the order of 1 μs.[32] Thus, in our case we can reasonably believe that it is possible to realize a superconducting device satisfying the constraint $T_\varphi > 10^4 t_{op}$. An open problem for the experimental realization of the physical system is represented by the coupling between a qubit and a single mode of a resonant cavity. We must take into account the typical dimensions of the SQUID chip with respect to the size of a high-Q superconducting cavity. In order to bypass this nontrivial technical problem we may use an experimental arrangement consisting of a chip placed inside a cavity made by two open mirrors[33] or we may think to integrate the Josephson device and a waveguide in the same chip.[34] Many groups are currently working in this field and we think (and hope) that these techniques will be of common use in the next few years. A most immediate solution is represented by the substitution of the resonant cavity by an LC resonator or by a large area current-biased Josephson junction. Several works taking into account this substitution and the fact that, as discussed in Sec. III, the Hamiltonian model for all these three systems may be expressed in terms of Eq. (10), make it possible to retain that this experiment may be realized with the currently available technologies.

ACKNOWLEDGMENTS

We wish to acknowledge C. Cosmelli, A. Vourdas, A. Konstadopoulou, and F. Chiarello for helpful discussions and F. Intravaia for his technical support. One of the authors (R.M.) acknowledges financial support from Finanziamento Progetto Giovani Ricercatori 1999, Comitato 02.

APPENDIX A

In this appendix, we give the analytical expressions for the eigenstates and eigenvalues of Hamiltonian (19) in the asymmetric case. In order to simplify the notation we introduce the following symbols:

$$G = \sqrt{4B^2\epsilon^2 + \hbar^2\omega_F^2}, \tag{A1}$$

$$Q_1 = \sqrt{4B^2\omega_F^2 + 2\hbar\omega_F(\hbar\omega_F - G)}, \tag{A2}$$

$$Q_2 = \sqrt{4B^2\omega_F^2 + 2\hbar\omega_F(\hbar\omega_F + G)}, \tag{A3}$$

$$P_1 = \hbar\omega_F + G, \tag{A4}$$

$$P_2 = \hbar\omega_F - G. \tag{A5}$$

The eigenvalues of the Hamiltonian (19) may be written down as follows:

$$\lambda_1 = \hbar\omega_F - \frac{Q_1}{2}, \tag{A6}$$

$$\lambda_2 = \hbar\omega_F + \frac{Q_1}{2}, \tag{A7}$$

$$\lambda_3 = \hbar\omega_F - \frac{Q_2}{2}, \tag{A8}$$

$$\lambda_4 = \hbar\omega_F + \frac{Q_2}{2}. \tag{A9}$$

The eigenstates $|u_1\rangle$, $|u_2\rangle$, $|u_3\rangle$, and $|u_4\rangle$ relative to the eigenvalues λ_1, λ_2, λ_3, and λ_4 respectively assume the following form:

$$|u_1\rangle = \frac{1}{\sqrt{n_1}}\left\{ -\frac{Q_1+P_2}{2B\Delta}|0-\rangle + \frac{P_1Q_1 - 4B^2\epsilon^2}{4B^2\Delta\epsilon}|1-\rangle - \frac{P_1}{2B\epsilon}|0+\rangle + |1+\rangle \right\}, \tag{A10}$$

$$|u_2\rangle = \frac{1}{\sqrt{n_2}}\left\{ \frac{Q_1-P_2}{2B\Delta}|0-\rangle - \frac{P_1Q_1 + 4B^2\epsilon^2}{4B^2\Delta\epsilon}|1-\rangle - \frac{P_1}{2B\epsilon}|0+\rangle + |1+\rangle \right\}, \tag{A11}$$

$$|u_3\rangle = \frac{1}{\sqrt{n_3}}\left\{ -\frac{Q_2+P_1}{2B\Delta}|0-\rangle + \frac{P_2Q_2 - 4B^2\epsilon^2}{4B^2\Delta\epsilon}|1-\rangle - \frac{P_2}{2B\epsilon}|0+\rangle + |1+\rangle \right\}, \tag{A12}$$

$$|u_4\rangle = \frac{1}{\sqrt{n_4}}\left\{ \frac{Q_2-P_1}{2B\Delta}|0-\rangle - \frac{P_2Q_2 + 4B^2\epsilon^2}{4B^2\Delta\epsilon}|1-\rangle - \frac{P_2}{2B\epsilon}|0+\rangle + |1+\rangle \right\}, \tag{A13}$$

where $1/\sqrt{n_i}$, with $i \equiv 1,2,3,4$, are the normalizing factors satisfying $\langle u_i|u_j\rangle = \delta_{ij}$. It is useful to expand the states $|0-\rangle$, $|1-\rangle$, $|0+\rangle$, and $|1+\rangle$ in terms of $|u_1\rangle$, $|u_2\rangle$, $|u_3\rangle$, and $|u_4\rangle$. Inverting Eqs. (A10)–(A13), we get

$$|0-\rangle = \frac{B\Delta}{(P_1-P_2)Q_1Q_2}[\sqrt{n_1}P_2Q_2|u_1\rangle - \sqrt{n_2}P_2Q_2|u_2\rangle - \sqrt{n_3}P_1Q_1|u_3\rangle + \sqrt{n_4}P_1Q_1|u_4\rangle], \tag{A14}$$

$$|1-\rangle = \frac{2B^2\Delta\epsilon}{(P_1-P_2)Q_1Q_2}[\sqrt{n_1}Q_2|u_1\rangle - \sqrt{n_2}Q_2|u_2\rangle - \sqrt{n_3}Q_1|u_3\rangle + \sqrt{n_4}Q_1|u_4\rangle], \tag{A15}$$

$$|0+\rangle = \frac{B\epsilon}{(P_1-P_2)Q_1Q_2}[\sqrt{n_1}(P_2-Q_1)Q_2|u_1\rangle - \sqrt{n_2}(P_2+Q_1)Q_2|u_2\rangle - \sqrt{n_3}(P_1-Q_2)Q_1|u_3\rangle + \sqrt{n_4}(P_1+Q_2)Q_1|u_4\rangle], \tag{A16}$$

$$|1+\rangle = \frac{1}{2(P_1-P_2)Q_1Q_2}[\sqrt{n_1}Q_2(P_1P_2+P_2^2-P_2Q_1 + 4B^2\epsilon^2)|u_1\rangle - \sqrt{n_2}\ Q_2(P_1P_2+P_2^2+P_2Q_1 + 4B^2\epsilon^2)|u_2\rangle - \sqrt{n_3}Q_1(P_1^2+P_1P_2-P_1Q_2 + 4B^2\epsilon^2)|u_3\rangle + \sqrt{n_4}Q_1(P_1^2+P_1P_2+P_1Q_2 + 4B^2\epsilon^2)|u_4\rangle]. \quad \text{(A17)}$$

APPENDIX B

In this section, we give the analytical expressions for the transition probabilities $P_2(t)$, $P_3(t)$, and $P_4(t)$ to the states $|1-\rangle$, $|0-\rangle$, and $|1+\rangle$ for a system in the asymmetric configuration and prepared at $t=0$ in the state $|0+\rangle$.

Exploiting Eqs. (20), (A14), (A15), and (A17), we write down these transition probabilities as

$$P_2(t) = |\langle 1-|0+\rangle_t|^2 = S^2\left\{\sum_{j=1}^{4} T_j^2 + 2T_1T_2\cos\frac{Q_1}{\hbar}t + 2T_3T_4\cos\frac{Q_2}{\hbar}t + 2[T_1T_3+T_2T_4]\cos\frac{(Q_1-Q_2)}{2\hbar}t + 2[T_2T_3+T_1T_4]\cos\frac{(Q_1+Q_2)}{2\hbar}t\right\}, \quad \text{(B1)}$$

where

$$T_1 = Q_2\frac{P_2-Q_1}{4B^2\epsilon\Delta}(-4B^2\epsilon^2+Q_1P_1), \quad \text{(B2)}$$

$$T_2 = Q_2\frac{P_2+Q_1}{4B^2\epsilon\Delta}(4B^2\epsilon^2+Q_1P_1), \quad \text{(B3)}$$

$$T_3 = Q_1\frac{-P_1+Q_2}{4B^2\epsilon\Delta}(-4B^2\epsilon^2+Q_2P_2), \quad \text{(B4)}$$

and

$$T_4 = Q_1\frac{P_1+Q_2}{4B^2\epsilon\Delta}(-4B^2\epsilon^2-Q_2P_2). \quad \text{(B5)}$$

Also

$$P_3(t) = |\langle 0-|0+\rangle_t|^2 = S^2\left\{\sum_{j=1}^{4} Z_j^2 + 2Z_1Z_2\cos\frac{Q_1}{\hbar}t + 2Z_3Z_4\cos\frac{Q_2}{\hbar}t + 2[Z_1Z_3+Z_2Z_4]\cos\frac{(Q_1-Q_2)}{2\hbar}t + 2[Z_2Z_3+Z_1Z_4]\cos\frac{(Q_1+Q_2)}{2\hbar}t\right\}, \quad \text{(B6)}$$

where

$$Z_1 = Q_2\frac{P_2-Q_1}{2B\Delta}(-P_2-Q_1), \quad \text{(B7)}$$

$$Z_2 = -Q_2\frac{P_2+Q_1}{2B\Delta}(-P_2+Q_1), \quad \text{(B8)}$$

$$Z_3 = Q_1\frac{-P_1+Q_2}{2B\Delta}(-P_1-Q_2), \quad \text{(B9)}$$

$$Z_4 = Q_1\frac{P_1+Q_2}{2B\Delta}(-P_1+Q_2), \quad \text{(B10)}$$

and

$$P_4(t) = |\langle 1+|0+\rangle_t|^2 = S^2\left\{\sum_{j=1}^{4} X_j^2 + 2X_1X_2\cos\frac{Q_1}{\hbar}t + 2X_3X_4\cos\frac{Q_2}{\hbar}t + 2[X_1X_3+X_2X_4]\cos\frac{(Q_1-Q_2)}{2\hbar}t + 2[X_2X_3+X_1X_4]\cos\frac{(Q_1+Q_2)}{2\hbar}t\right\}, \quad \text{(B11)}$$

where

$$X_1 = Q_2(P_2-Q_1), \quad \text{(B12)}$$

$$X_2 = -Q_2(P_2+Q_1), \quad \text{(B13)}$$

$$X_3 = Q_1(-P_1+Q_2), \quad \text{(B14)}$$

$$X_4 = Q_1(P_1+Q_2). \quad \text{(B15)}$$

*Electronic address: rosanna@fisica.unipa.it

[1] A.J. Leggett, S. Chakravarty, A.T. Dorsey, M.P.A. Fisher, A. Garg, and W. Zwerger, Rev. Mod. Phys. **59**, 1 (1987).

[2] D.P. Di Vincenzo, Science **270**, 255 (1995); C.H. Bennet and D.P. Di Vincenzo, Nature (London) **404**, 247 (2000).

[3] R. Rouse, S. Han, and J.E. Lukens, Phys. Rev. Lett. **75**, 1614 (1995); R.F. Voss and R.A. Webb, *ibid.* **47**, 265 (1981); J.M. Martinis, M.H. Devoret, and J. Clarke, Phys. Rev. B **35**, 4682 (1987).

[4] J. Clarke, A.N. Cleland, M.H. Devoret, D. Esteve, and J.M. Martinis, Science **239**, 992 (1988).

[5] J. Friedman, V. Patel, W. Chen, S.K. Tolpygo, and J.E. Lukens, Nature (London) **406**, 43 (2000).

[6] C.H. van der Wal, A.C.J. ter Haar, F.K. Wilhelm, R.N. Schouten, C.J.P.M. Harmans, T.P. Orlando, S. Lloyd, and J.E. Mooij, Science **290**, 773 (2000).

[7] U. Weiss, *Quantum Dissipative Systems* (Word Scientific, Singapore, 1999).

[8] Y. Makhlin, G. Schön, and A. Shnirman, Rev. Mod. Phys. **73**, 357 (2001).

[9] K.K. Likharev, *Dynamics of Josephson Junctions and Circuits* (Gordon and Breach Science, London, 1986).

[10] Y. Nakamura, Yu.A. Pashkin, and J.S. Tsai, Nature (London) **398**, 786 (1999).

[11] Y. Nakamura, Yu.A. Pashkin, and J.S. Tsai, Phys. Rev. Lett. **87**, 246601 (2001).
[12] D. Vion, A. Aassime, A. Cottet, P. Joyez, H. Pothier, C. Urbina, D. Esteve, and M.H. Devoret, Science **299**, 886 (2002).
[13] J.M. Martinis, S. Nam, J. Aumentado, and C. Urbina, Phys. Rev. Lett. **89**, 117901 (2002).
[14] F. Plastina and G. Falci, cond-mat/0206586 (unpublished).
[15] F.W.J. Hekking, O. Buisson, F. Balestro, and M.G. Vergniory, cond-mat/0201284 (unpublished).
[16] J.M. Raimond, M. Brune, and S. Haroche, Rev. Mod. Phys. **73**, 565 (2001).
[17] J.I. Cirac and P. Zoller, Phys. Rev. Lett. **74**, 4091 (1995).
[18] R. Migliore, A. Messina, and A. Napoli, Eur. Phys. J. B **13**, 585 (2000).
[19] R. Migliore, A. Messina, and A. Napoli, Eur. Phys. J. B **22**, 111 (2001).
[20] W.A. Al-Saidi and D. Stroud, Phys. Rev. B **65**, 014512 (2002).
[21] O. Buisson and F.W.J. Hekking, in *Macroscopic Quantum Coherence and Quantum Computing 2000*, edited by D.V. Averin *et al.* (Kluwer, Dordrecht, New York, 2001).
[22] J. Diggins, T.D. Clark, H. Prance, R.J. Prance, T.P. Spiller, J. Ralph, and F. Brouers, Physica B **215**, 367 (1995).
[23] M.J. Everitt, P. Stiffell, T.D. Clark, A. Vourdas, J.F. Ralph, H. Prance, and R.J. Prance, Phys. Rev. B **63**, 144530 (2001); M.J. Everitt, T.D. Clark, P. Stiffell, H. Prance, R.J. Prance, A. Vourdas, and J.F. Ralph, *ibid.* **64**, 184517 (2001).
[24] R. Migliore and A. Messina, cond-mat/0203529 (unpublished).
[25] Y. Yu, S. Han, X. Chu, S. -I Chu, and Z. Wang, Science **296**, 889 (2002).
[26] Y. Makhlin, G. Schön, and A. Shnirman, Physica C **368**, 276 (2002).
[27] Z. Zhou, Shih-I Chu, and S. Han, Phys. Rev. B **66**, 054527 (2002).
[28] A.J. Leggett, J. Phys.: Condens. Matter **14**, R415 (2002).
[29] F. Chiarello, Phys. Lett. A **277**, 189 (2000).
[30] P. Carelli, M.G. Castellano, F. Chiarello, C. Cosmelli, R. Leoni, F. Sciamanna, and G. Torrioli, in *Proceedings of EuroConference on the Physics and Applications of the Intrinsic Josephson Effect, 2002*, edited by P. Müller (Universität Erlangen, Nürnberg, 2002). On-line in http://www.physik.uni-erlangen.de/PI3/intrinsic/proceedings.html
[31] J. Preskill, Proc. R. Soc. London, Ser. A **454**, 385 (1998).
[32] C. Cosmelli, P. Carelli, M.G. Castellano, F. Chiarello, R. Leoni, B. Ruggiero, P. Silvestrini, and G. Torrioli, J. Supercond. **12**, 773 (1999).
[33] G.R. Guthöherlein, M. Keller, K. Hayasaka, W. Lange, and H. Walther, Nature (London) **414**, 49 (2001).
[34] M. Cirillo (private communication).